PERGAMON

International Journal of Heat and Mass Transfer 41 (1998) 3203–3211

International Journal of HEAT and MASS TRANSFER

Conjugate natural convection from a vertical heated slab

Shigeo Kimura*, Atsushi Okajima, Takahiro Kiwata

Department of Mechanical Systems Engineering, Faculty of Engineering, Kanazawa University, 2-40-20 Kodatsuno, Kanazawa 920-8667, Japan

Received 8 September 1997; in final form 16 January 1998

Abstract

Conjugate natural convection heat transfer from a vertical plate has been investigated analytically and experimentally. Assuming the existence of vertically averaged interfacial temperature between plate and fluid, it is shown that there is a unique nondimensional parameter to characterize the problem. The interfacial temperature is obtained as a root of 5th order polynomial for laminar natural convection, and it is presented as a function of the conjugate parameter. For turbulent convection it is also shown that the polynomial becomes 4th order. A simple expression for the average heat transfer is given as a function of conjugate parameter and the apparent Rayleigh number defined by an overall temperature difference. An experiment, using a water vessel with a heating plate on a side wall, was carried out in order to test a proposed theory for the heat transfer. Three different materials, copper, stainless steel and ceramics, were used as a conductive slab. The measured average heat transfer rates are in good agreement with the theory.

Nomenclature

A heat transfer area of slab
a slab thickness
C constant in heat transfer correlation
g gravitational acceleration
H slab height
k thermal conductivity ratio, and also thermal conductivity of slab or fluid with subscripts 's' and 'f'
Nu average Nusselt number
Pr Prandtl number
Q dissipated electric power
Ra Rayleigh number
T temperature
y vertical coordinate
z nondimensional temperature; $z = \theta^{1/3}$ or $z = \theta^{1/4}$.

Greek symbols

α thermal diffusivity of fluid
β volumetric thermal expansion coefficient
δ thermal boundary layer thickness
θ nondimensional temperature
λ geometric aspect ratio
ν kinematic viscosity
σ nondimensional conjugate parameter.

Subscripts

b slab–fluid interface temperature
H heated surface of slab
C cold fluid
s slab
f fluid.

1. Introduction

Natural convection from a heated vertical plate is one of the most basic configurations that arise in free convection heat transfer problems. Although an isothermal condition of the heated plate is commonly assumed for evaluating the local and average heat transfer coefficients and the associated convecting fluid motion, the condition cannot be always realized in reality. The constant temperature condition of the heated plate is true only when the solid thermal conductivity is much greater than that of fluid. In general, however, this condition cannot be satisfied, and the fluid–solid interfacial temperature is only determined by a balance between the thermal resistance of fluid and that of solid plate or slab. Since the

* Corresponding author.

0017–9310/98 $19.00
PII: S0017–9310(98)00063–5

thermal resistance of fluid adjacent to the plate depends upon the thickness of thermal boundary layer formed along the vertical plate or slab, it cannot be prescribed beforehand. Rather, the solid–fluid interfacial temperature is obtained as a part of the solution of conduction-convection conjugated problem.

Conjugate heat transfer problems arise in many practical applications; one of such examples demonstrates a critical nature of this problem in modern key-technologies. In the mid-seventies in the piping systems of nuclear reactors it has been ascertained that natural circulation induces thermal stresses in the pipe walls and lead to critical structural damage [1]. In these situations the thermal stresses induced depend on the temperature field within the solid wall, which is simply a result of thermal coupling between two adjacent media, fluid and solid wall. There have been several works on this convection–conduction coupling. Notably, heat transfer enhancement by extended surface, such as fins, is one example that falls into this category and has been investigated extensively (see Holman [2] and Bejan [3], for instance). Kelleher and Yang [4] worked on a heat transfer problem from a vertical slab heated by internal heat generation. Zinnes [5] studied a case where a localized heat generation is imbedded in a vertical plate. Rotem [6] worked on a conjugate natural convection from a horizontal cylinder. A similar problem has been numerically investigated recently by Kimura and Pop [7]. The latter also provided an approximate analytical solution for the average boundary temperature and the average heat transfer coefficient, which is extremely easy to evaluate, but accurate enough for most engineering applications. Further Lock and Ko [8] looked at a heat transfer problem between two fluid reservoirs at different temperatures when they are partitioned by a conductive wall. Later Anderson and Bejan [9] developed an analytical solution regarding heat transfer and convecting fluid motion, which is based on the Oseen type approximation proposed by Gill [10]. The same problem was also investigated theoretically and experimentally by Viskanta and Lankford [11].

Probably a most relevant work to the present one has been first advanced by Miyamoto et al. [12] who provided both experimental and numerical results and an analytical solution valid for a boundary layer regime along a heated vertical plate either by constant temperature or by constant flux. In a conjugated heat transfer problem a difficulty arises when one matches a conductive solution in the vertical plate and a nonlinear convection solution in the fluid region at the interfacial boundary. They overcome this difficulty by approximating the interfacial temperature as a polynomial of vertical coordinate variable. Subsequently, Timma and Padet [13], and Pozzi and Lupo [14] developed analytical solutions by assuming a thin heated slab so that conduction within the solid is one-dimensional. Merkin and Pop [15] have concluded that the thin plate approximation only leaves the Prandtl number as a relevant nondimensional parameter in the conjugate natural convection problem. The most general case of conjugate natural convection, however, must include both finite thickness and length of the heated plate as relevant parameters. From this argument Vynnycky and Kimura [16] made a most general formulation and provided both local and average heat transfer results when a vertical plate is heated from the behind at constant temperature. It should be mentioned that the solution by Vynnycky and Kimura [16] does not require any approximation on the interfacial boundary temperature profile.

Despite a rather substantial body of publications regarding conjugate natural convection along a vertical plate or slab, experimental work is very limited. Only a paper by Miyamoto et al. [12], which provides a set of experimental heat transfer data when the plate is heated by constant flux and the heat is transferred to the adjacent air ($Pr = 0.7$) comes to the present authors' mind. On the other hand, Vynnycky and Kimura [16] proposed easily-obtainable formulae for the average interfacial boundary temperature and the average Nusselt number. The purpose of the present paper, therefore, is two-fold; one is to provide a conjugate Nu–Ra correlation when the plate or slab is heated from behind by a constant temperature and facing to a reservoir filled with water ($Pr = 7$), and the other is to test a simple theory on the average heat transfer characteristics developed by Vynnycky and Kimura [16].

2. One-dimensional approximate analysis

2.1. Laminar flow regime

It is a well established fact that a thin thermal boundary layer is formed along the heated vertical plate when the Rayleigh number is large. Therefore, it can be postulated the existence of a vertically averaged temperature field, which is then used to capture a major feature of the temperature field and the resulting heat transfer rate. We illustrate a physical model of the present problem and its coordinate system in Fig. 1. A heat conductive slab is positioned vertically and heated from behind at a constant temperature T_H. The other side of the slab is facing to a fluid reservoir of constant temperature T_C. The slab is sandwiched between two perfectly-insulated plates, and its upper and lower surfaces are, therefore, thermally insulated. The vertical and horizontal dimensions of the slab are H and a, respectively. The thermal conductivities of the slab and the fluid are k_s and k_f. At steady state we have a thermal boundary layer developed next to the conductive slab. The thickness of the boundary layer is denoted by δ in the figure. Defining the vertically-averaged solid–fluid interface temperature as

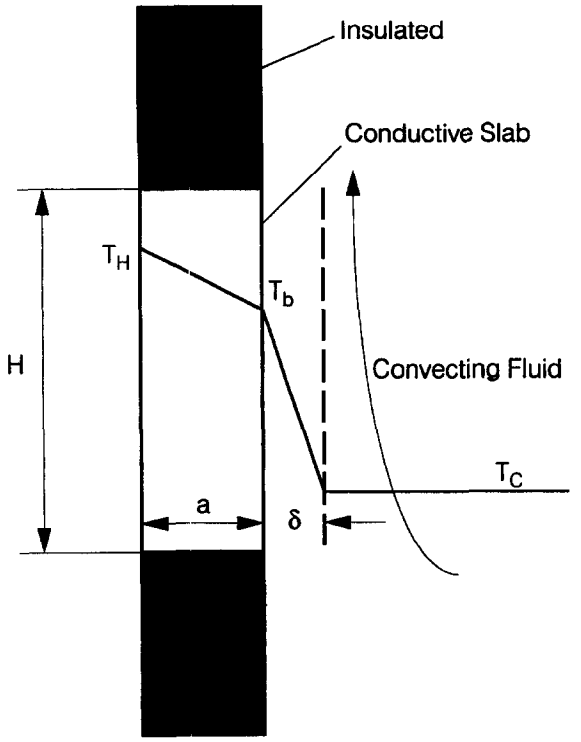

Fig. 1. Schematic diagram of conjugate natural convection from a vertical slab.

$$T_b = \frac{1}{H}\int_0^H T(0,y)\,dy \tag{1}$$

we can write a one-dimensional heat balance at the interface boundary.

$$\frac{k_s(T_H - T_b)}{a} = \frac{k_f(T_b - T_C)}{\delta}. \tag{2}$$

In equation (2) linear temperature profiles within the slab and the thermal boundary layer are assumed. The thermal boundary layer thickness δ can be related with the Rayleigh number Ra through a heat transfer correlation for a vertical heated plate when the Prandtl number Pr is large;

$$\delta/H = C^{-1}\,Ra^{-1/4} \tag{3}$$

where C is a constant whose value is $C = 0.671$, and Ra is defined by an actual temperature difference to drive convection $T_b - T_C$ and the slab height H (for example, see Bejan [3]). It should be noted that the boundary layer thickness δ does not measure the real thermal boundary layer thickness, rather it reflects a fictitious value that correctly measures a mean heat transfer rate when a linear temperature profile is assumed within the boundary layer. Equation (2) may be put in a dimensionless form by dividing through the maximum temperature difference within the system $T_H - T_C$, and substituting equation (3) for δ

$$\frac{k_s(1-\theta)}{\alpha} = \frac{k_f\theta^{5/4}C\,Ra^{1/4}}{H} \tag{4}$$

where θ is the dimensionless interface temperature defined by

$$\theta = \frac{T_b - T_C}{T_H - T_C}. \tag{5}$$

Equation (4) is quintet polynomial equation for $z = \theta^{1/4}$, and it should be noted that Ra in equation (4) is the apparent Rayleigh number defined by an overall temperature difference $T_H - T_C$. Therefore, we obtain a quintet algebraic equation for z with a single parameter σ.

$$\sigma z^5 + z^4 - 1 = 0 \tag{6}$$

where

$$\sigma = \frac{\lambda C\,Ra^{1/4}}{k}, \quad k = \frac{k_s}{k_f}, \quad \lambda = \frac{a}{H}. \tag{7}$$

The σ is a measure of thermal resistance of the solid slab relative to a neighboring fluid. Equation (6) does not possess a closed form solution, although it is possible to obtain the properties of the solution before finding a root numerically. First, asymptotic analysis indicates that

$$\theta \approx 1-\sigma, \quad \text{when } \sigma \ll 1 \tag{8}$$

$$\theta \approx \sigma^{-4/5}, \quad \text{when } \sigma \gg 1. \tag{9}$$

Since equation (6) is a 5th-order polynomial, there are five roots all together. However, the equation has only two turning points, and it is obvious that it has three real roots. Furthermore, since it has a negative value at $z = 0$ and a positive one at $z = 1$, we can deduce that only one of three lies in the range $0 \leqslant z \leqslant 1$, also considering the fact that the first derivative is positive in this range.

In the light of this analysis, the unique solution for the interfacial temperature as a function of σ can be found easily using a Newton–Raphson technique. The results are shown graphically in Fig. 2. As expected from equations (8) and (9), the interfacial temperature decreases monotonically as σ increases. Particularly when $\sigma \leqslant 10$, it decreases sharply from 1 to around 0.2, and after that the decay is less dramatic.

Once the solid–fluid interfacial temperature is obtained, the mean Nusselt number can be calculated from a correlation for a heated vertical plate. Therefore, the mean Nusselt number may be written as

$$Nu = C\,Ra^{1/4}\theta^{5/4}. \tag{10}$$

It should be noted that the Rayleigh number is again an apparent one as those in equations (4) and (7) and the Nusselt number is defined by

$$Nu = \frac{q''H}{k_f(T_H - T_C)} \tag{11}$$

where q'' is a mean heat flux per unit area.

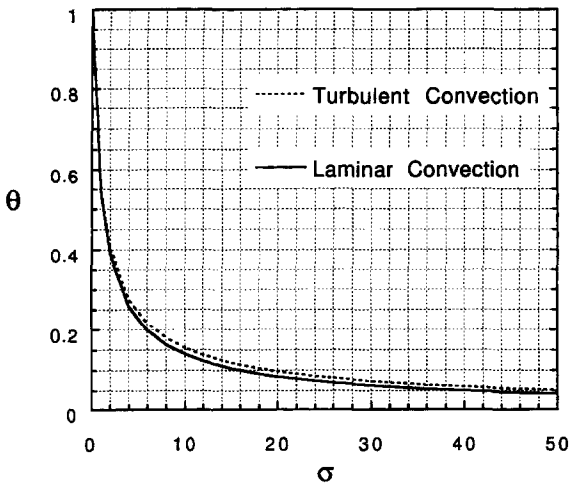

Fig. 2. Dimensionless slab–fluid interface temperatures for both laminar and turbulent flows as a function of σ.

The case for $Pr \ll 1$, and $Ra\,Pr \gg 1$ proceeds in a similar way, except that the boundary layer thickness now measured by

$$\delta/H = C^{-1}(Ra\,Pr)^{-1/4}. \tag{12}$$

Therefore, a unique parameter σ for $Pr \ll 1$ becomes

$$\sigma = \frac{\lambda C(Ra\,Pr)^{1/4}}{k} \tag{13}$$

where $C = 0.8$ in this case (see Bejan [3]). Otherwise, the former argument is exactly applicable for the small Prandtl number problem.

2.2. Turbulent flow regime

At a sufficiently large Rayleigh number the convecting flow eventually becomes turbulent. For a heated vertical plate the transition from laminar flow to turbulence takes place around $Ra = 10^9$. However, it should be noted that this transition criteria is for an isothermal vertical plate. For the present problems the critical Rayleigh number may be different. In the presence of turbulent in the boundary layer the heat transfer rate has been measured experimentally and correlated as a function of Ra. For a fluid of $Pr \gg 1$ the following equation has been proposed

$$\delta/H = C^{-1}\,Ra^{-1/3} \tag{14}$$

with $C = 0.15$ (see Bejan [3] and Churchill and Chu [17]). Exactly the same procedure as in the laminar case may be carried out for turbulent convection. A polynomial equation for turbulent case, corresponding to equation (6) for laminar flow, now becomes

$$\sigma z^4 + z^3 - 1 = 0 \tag{15}$$

where the dimensionless interfacial temperature is given by $\theta = z^3$. The conjugate parameter σ for turbulent convection is defined by

$$\sigma = \frac{\lambda C\,Ra^{1/3}}{k}. \tag{16}$$

Equation (15) shares a similar property with equation (6); there is a unique root lying in the range of $0 \leqslant z \leqslant 1$ for any value of σ. The numerical values of θ obtained by solving equation (15) are plotted in Fig. 2 together with laminar case. The interface temperature monotonically decreases as σ increases; the trend is very close to that for laminar convection. The mean Nusselt number is calculated using equation (17) in the same way as it is for laminar flow,

$$Nu = C\,Ra^{1/3}\,\theta^{4/3}. \tag{17}$$

The definitions of σ and the formulae to compute the average Nusselt numbers for laminar and turbulent convection, and for large and small Prandtl number cases are summarized in Table 1.

3. Experimental setup and procedure

An experimental apparatus was built in order to examine the above theoretical development. A water vessel whose dimensions are $300 \times 300 \times 500$ mm was built with acrylic plates, which serves as a fluid reservoir. A heated slab is placed at the midheight on one of the 500 mm-high side walls. The conductive slabs have the area dimension of 70 mm (height) $\times$ 200 mm (width) and a thickness of 21 mm. The vertical dimension of the slab essentially restricts the attainable maximum Rayleigh number, which appears to be an order of 10^8 (based on the temperature difference $T_b - T_C$). Therefore, convective flows are expected to be laminar over the heated surface. Three different conductive materials are used; they are copper ($k_s = 386$ W m^{-1} K^{-1}), stainless steel ($k_s = 16$ W m^{-1} K^{-1}) and ceramics ($k_s = 1.7$ W m^{-1} K^{-1}). Except for the copper slab they are heated by two electric heaters via a 6 mm copper plate in order to maintain the heated surface at a constant temperature. The temperature field is measured by thermocouples. All together eleven thermocouples are mounted in the heated slab in order to monitor the temperatures at both surfaces. The temperature

Table 1
Conjugate parameters and average Nusselt numbers

	Pr	σ	C	Nu
Laminar	$Pr \gg 1$	$\lambda C\,Ra^{1/4}/k$	0.67	$C\,Ra^{1/4}\,\theta^{5/4}$
	$Pr \ll 1$	$\lambda C(Pr\,Ra)^{1/4}/k$	0.8	$C(Pr\,Ra)^{1/4}\,\theta^{5/4}$
Turbulent	$Pr \gg 1$	$\lambda C\,Ra^{1/3}\,k$	0.15	$C\,Ra^{1/3}\,\theta^{4/3}$
	$Pr \ll 1$	$\lambda C(Pr\,Ra)^{1/3}/k$	0.19	$C(Pr\,Ra)^{1/3}\,\theta^{4/3}$

of water is also measured by a thermocouple probe mounted on a rack-pinion positioning system. A schematic in Fig. 3 illustrates the water vessel and a layout of the heated slab.

The heat transfer rate is measured by electric power dissipated at electric heaters mounted behind the slabs. The heat transfer rate is presented by a Nusselt–Rayleigh correlation, where the Rayleigh number again refers to the apparent Rayleigh number based on overall temperature difference. The mean Nusselt number is defined by equation (11) and measured from an average heat flux per unit area through the heated slab,

$$Nu = \frac{QH}{Ak_f(T_H - T_C)} \tag{18}$$

where Q and A are a dissipated power at the electric heaters and the heat transfer area of the slab, respectively.

Since there must be a leakage of heat, particularly from behind the heaters through insulation material, we conducted a series of tests in order to estimate the heat leak by supplying a very small amount of power to the heaters for the water-drained vessel, where the surface of the conductive plate is also insulated by glass wool. The temperature rise at a steady state is then monitored for several different input powers, and the dissipated powers are plotted against the temperature differences between the plate and the ambient room temperature. It appears that the heat leak estimated increases as the conductive plate temperature becomes large, but it is roughly within an order of 10–15% of the total power dissipated at the heaters.

A flow visualization was also conductive in order to look at fluid dynamic processes during a steady convective state. A pH indicator method demonstrated by Baker [18] for slow fluid motion was applied to the present experiments. For the visualization purpose the vessel was filled with aquatic solution of thymalblue, and 0.05 mm-diameter stainless steel wires are put straight in the mid-vertical plane. After steady convection is established, a d.c. voltage is impressed between the wires, one (positive) of which colors the neighboring fluid dark-blue. The colored fluid are then swept by moving fluid, and forms streak lines. The method was successfully applied to visualize convecting flow structures in the present water vessel.

4. Experimental results

4.1. Heat transfer

As described above the heat transfer rates were measured by monitoring powers dissipated by electric heaters. In order to examine a performance of the experimental apparatus we first used a copper plate as a conductive slab. The surface temperatures of the slab are measured by imbedded thermocouples at positions 1 mm away from the front boundary. After the heater was switched on, the slab–fluid boundary temperature rise was monitored every one minute. A steady state was achieved in 20–40 min depending upon the Rayleigh number. The Rayleigh number and the Nusselt number are defined by temperature difference between the slab surface and the directly opposing vessel wall. Due to a large heat conductivity of copper uniform temperatures at the surface were observed. The measured nondimensional heat transfer rates (Nusselt number) are plotted against the Ray-

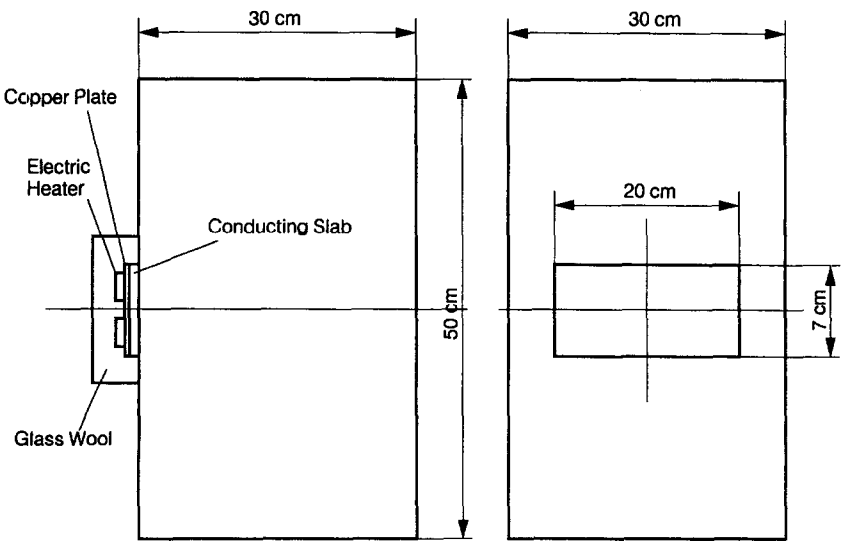

Fig. 3. Sketch of experimental apparatus.

leigh number together with the similarity solution (Bejan [3]) in Fig. 4. As it is seen in the figure, the experimental results agree well with the similarity solution: the differences between the two fall within 12%. This proves that the experimental apparatus works properly for the purpose of heat transfer measurements.

Next we installed alternatively stainless steel and ceramics as a conductive slab in order to realize a conduction–convection conjugate heat transfer problem. Since those materials have lower thermal conductivities than copper, it is expected that the heat transfer rates decrease significantly, and the slab–fluid boundary temperatures also diminish. A steady state was determined again by monitoring a slab–fluid boundary temperature. A time required for steady state is generally greater than that for copper, and takes about 1–4 h, reflecting smaller thermal diffusivities of stainless steel and ceramics. When a required period of time for steady state became greater than 1 h, a slight temperature rise at midheight of the opposing wall was observed. The opposing wall temperature also fluctuates by a room temperature variation with time. However, a temperature difference between the two kept a nearly constant value once a steady state was established.

The Nusselt–Rayleigh correlations obtained for the latter two cases are shown in Figs. 5 and 6 together with theoretical predictions based on the one-dimensional theory developed in the preceding section. Again it is clear that the experimental results agree well with the theory: the differences are within 16%. The ceramic slab drops the heat transfer rates by a factor of 10 in comparison with the copper case, and the stainless steel lies somewhere between the two. But, considering the fact that ceramics is more than 200 times less thermally conductive than copper, the factor of 10 obtained for the heat transfer difference between the two is small, and it indicates that the convective process gives a significant contribution for determining the overall conjugate heat transfer rate.

The slab–fluid boundary temperatures (surface temperature) are also measured by nine thermocouples that

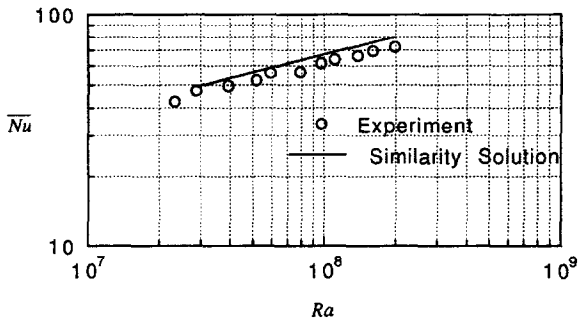

Fig. 4. Average Nusselt number against Rayleigh number for copper slab; (similarity solution vs. experimental results).

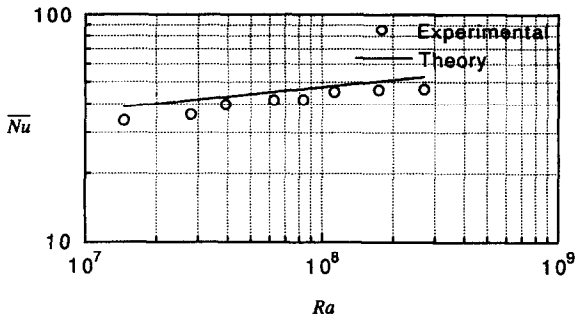

Fig. 5. Average Nusselt number against apparent Rayleigh number for stainless steel slab; (theory vs. experimental results).

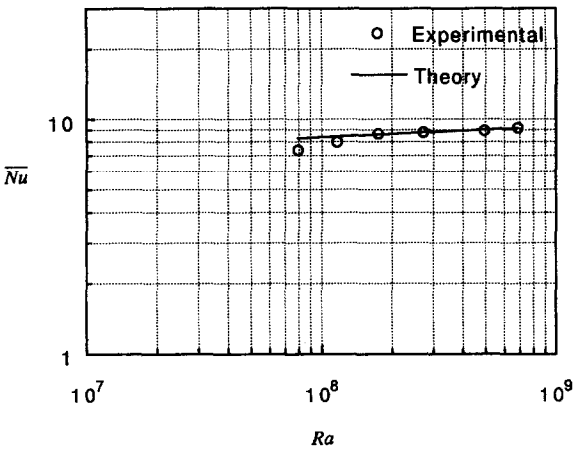

Fig. 6. Average Nusselt number against apparent Rayleigh number for ceramic slab; (theory vs. experimental results).

are imbedded in the slab. The temperature rises in general in the upward direction. A few examples of the vertical boundary temperature variation T_b are listed in Table 2. The vertical temperature variations are about 40–50% of $T_b - T_C$ (about 20% of $T_H - T_C$) in the present experiments. The average boundary temperature is determined by taking the mean of the measured nine values. In Fig. 7 the nondimensional boundary temperatures obtained by our experiments are plotted together with the theor-

Table 2.
Vertical variations of T_b [°C] for ceramic plate [$k = 1.7$ W m^{-1} K^{-1}]

Ra	T_H	T_C	T_b (top)	T_b (middle)	T_b (bottom)
7.9×10^7	31.9	19.8	26.0	24.8	24.2
2.7×10^8	51.1	20.9	34.7	31.6	29.0
6.9×10^8	73.8	25.6	47.6	42.5	38.8

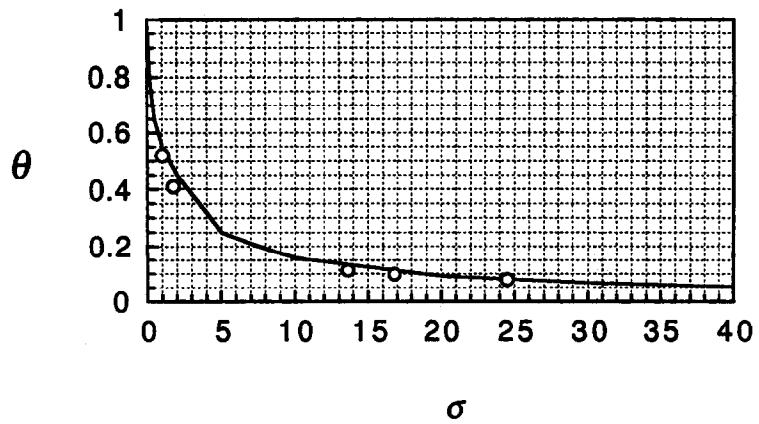

Fig. 7. Averaged dimensionless solid–fluid boundary temperature as a function of σ; theory (solid line) vs. experimental results (blank circles).

etical curve for laminar convection given in Fig. 2. The two plots for small values of σ are taken from stainless steel plate, and the rest are from ceramic plate. Again the experimental data fall within 15% of the theoretical curve.

4.2. Flow structure and temperature field in convecting water

Flow structures and temperature fields in convecting water for a few representative cases were obtained via a flow visualization technique based on pH indicator method and thermocouple probe. The temperature measurements revealed a presence of three distinctive regimes (Fig. 8). Obviously a thermal boundary layer adjacent to a heated slab was evident, where a large horizontal temperature gradient was measured. A region, extending out horizontally from the edge of the vertical thermal boundary layer and vertically above the lower edge of the slab, was thermally stratified. The aforementioned two regions lay above a nearly isothermal body of cold water. The flow structure was visualized by a pH indicator method (Fig. 9). Streaks of dark-color released from three stainless steel wires show a main lateral flow toward a heated surface; a thickness (or height) of the flow is roughly equal to the height of the slab. Above that four or five laterally advancing flows one above another with smaller velocities and changing their directions alternatively with height were observed. Below the main lateral flow it was found that water was essentially stagnant. A picture of flow and temperature field described above was independent of Rayleigh number and slab material.

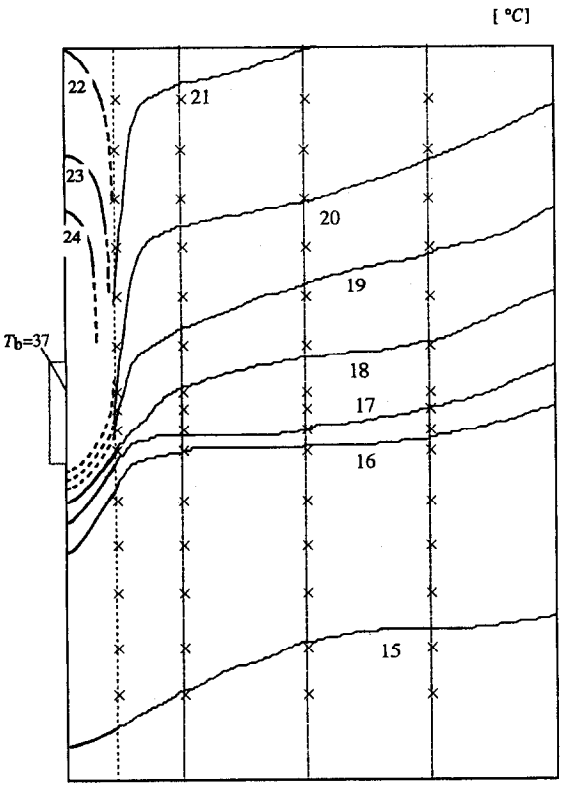

Fig. 8. Sketch of a steady temperature field in the water vessel (copper plate, $T_b = 37°C$, $Ra = 1.48 \times 10^8$). Crosses indicate positions where the temperature measurements took place.

5. Conclusion

A conjugate natural convection from a vertical slab has been studied analytically and experimentally. Assuming a vertically-averaged slab–fluid interface temperature, a simple 5th- or 4th-order polynomial equation is deduced for the unknown interface temperature, depending upon whether convecting flow is in laminar or turbulent

(a) t = 2 [min.]

(b) t = 4 [min.]

Fig. 9. Steady state convecting flow patterns visualized by pH indicator method for $Ra = 1.1 \times 10^8$ (copper plate): elapsed times are (a) 2 min; (b) 4 min.

regime. The polynomial involves a single nondimensional parameter, which is made of the apparent Rayleigh number, slab to fluid thermal conductivity ratio and the slab aspect ratio. The solutions for the interface temperature are graphically presented as a function of this dimensionless parameter σ. The mean Nusselt number is then derived based on the obtained interface temperature. It should be noted that despite its approximate nature the analytical solution requires all the parameters present in the system and can be expected to work for a wide range of parameters.

A series of experiments have been conducted using three different slab materials and water as a working fluid. The mean heat transfer rates measured experimentally are well compared with analytical predictions based on the one-dimensional theory. Flow visualization and temperature measurement reveals three distinctive regions, namely a boundary layer regime adjacent to a heated slab, a temperature stratified regime and a body of stagnate cold water.

Acknowledgements

The present authors are grateful to Mr Masatoshi Kouno for conducting experimental measurements and to Mr Masato Nishida for various technical supports.

References

[1] Hong SW. Natural circulation in horizontal pipes. Int J Heat Mass Transfer 1977;20:685–91.
[2] Holman JP. Heat Transfer. 4th ed. New York: McGraw-Hill, 1976.
[3] Bejan A. Convection Heat Transfer. New York: Wiley-Interscience, 1984.
[4] Kelleher MD, Yang KT. A steady conjugate heat transfer problem with conduction and free convection. Appl Sci Res 1967;17:240–68.
[5] Zinnes AE. The coupling of conduction with laminar convection from a vertical plate with arbitrary surface heating. J Heat Transfer 1970;92:528–35.
[6] Rotem Z. Conjugate free convection from horizontal conducting circular cylinders. Int J Heat Mass Transfer 1972;15:1679–93.
[7] Kimura S, Pop I. Conjugate free convection from a circular cylinder in a porous medium. Int J Heat Mass Transfer 1992;35:3105–13.
[8] Lock GSH, Ko RS. Coupling through a wall between two free convective systems. Int J Heat Mass Transfer 1973;16:2087–96.
[9] Anderson R, Bejan A. Natural convection on both sides of vertical wall separating fluids at different temperatures. J Heat Transfer 1980;102:630–5.
[10] Gill AE, The boundary-layer regime for convection in a rectangular cavity. J Fluid Mechanics 1966;26:515–36.
[11] Viskanta R, Lankford DW. Coupling of heat transfer

between two natural convection systems separated by a vertical wall. Int J Heat Mass Transfer 1981;24: 1171–7.

[12] Miyamoto M, Sumikawa J, Akiyoshi T, Nakamura T. Effects of axial heat conduction in a vertical plate on free convection heat transfer. Int J Heat Mass Transfer 1980;23:1545–53.

[13] Timma J, Padet J-P. Etude theorique du couplage convection–conduction en convection libre laminaire sur une plaque plane verticale. Int J Heat Mass Transfer 1985;28:1097–104.

[14] Pozzi A, Lupo M. The coupling of conduction with laminar natural convection along a flat plate. Int J Heat Mass Transfer 1988;31:1807–14.

[15] Merkin JK, Pop I. Conjugate free convection on a vertical surface. Int J Heat Mass Transfer 1996;39:1527–34.

[16] Vynnycky M, Kimura S. Conjugate free convection due to a heated vertical plate. Int J Heat Mass Transfer 1996;39:1067–80.

[17] Churchill SW, Chu HHS. Correlating equations for laminar and turbulent free convection from a vertical plate. Int J Heat Mass Transfer 1975;18:1323–9.

[18] Baker DJ. A technique for the precise measurement of small fluid velocities. J Fluid Mechanics 1966;26:573–5.